

Improvement in Titanium Complexes Bearing Schiff Base Ligands in the Ring-Opening Polymerization of *L*-Lactide: A Dinuclear System with Hydrazine-Bridging Schiff Base Ligands

Hsi-Ching Tseng,[†] Hsing-Yin Chen,[†] Yen-Tzu Huang,[†] Wei-Yi Lu,[‡] Yu-Lun Chang,^{†,§} Michael Y. Chiang,^{†,§} Yi-Chun Lai,[†] and Hsuan-Ying Chen^{*,†}

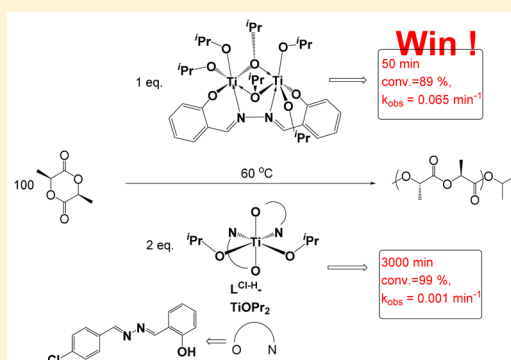
[†]Department of Medicinal and Applied Chemistry, Kaohsiung Medical University, Kaohsiung 80708, Taiwan R.O.C.

[‡]Department of Chemistry, National Chung Hsing University, Taichung 402, Taiwan R.O.C.

[§]Department of Chemistry, National Sun Yat-Sen University, Kaohsiung 804, Taiwan R.O.C.

S Supporting Information

ABSTRACT: A series of titanium (Ti) complexes bearing hydrazine-bridging Schiff base ligands were synthesized and investigated as catalysts for the ring-opening polymerization (ROP) of *L*-lactide (LA). Complexes with electron withdrawing or steric bulky groups reduced the catalytic activity. In addition, the steric bulky substituent on the imine groups reduced the space around the Ti atom and then reduced LA coordination with Ti atom, thereby reducing catalytic activity. All the dinuclear Ti complexes exhibited higher catalytic activity (approximately 10–60-fold) than mononuclear $L^{Cl-H}-TiOPr_2$ did. The strategy of bridging dinuclear Ti complexes with isopropoxide groups in the ROP of LA was successful, and adjusting the crowded heptacoordinated transition state by the bridging isopropoxide groups may be the key to our successful strategy.



1.0. INTRODUCTION

Poly(lactide) (PLA) is an accepted biopolymer designed to resolve the pollution problem caused by petrochemical plastics. It is also a common biomaterial in various fields such as MRI contrast agent,^{1a} humidity detection,^{1b} nanocomposites,^{1c} cell/tissue antiadhesion,^{1d} blood circulation,^{1e} drug delivery,^{1f} bone replacement,^{1g} tissue engineering,^{1h–m} and biomedical application^{1n,s} because of its biodegradability, biocompatibility, and permeability. Ring-opening polymerization (ROP) is the main method of synthesizing PLA with various metal catalysts.² Because of the problem of cytotoxic metal residues in PLA, the use of a noncytotoxic metal such as titanium (Ti)³ has been researched extensively with regard to lactides polymerization. Ligands are crucial for designing organometallic catalysts because of their ability to improve reactivity and selectivity. A study on the creation of Ti complexes^{3j} bearing Schiff base ligands reported that the different steric effects of these ligands altered the coordinated form with various catalytic activities of *L*-lactide (LA) and ϵ -caprolactone polymerizations as shown in Figure 1.

Bochmann^{3k} and Lin^{3l} both reported that the catalytic activity of heterobimetallic Ti complexes bearing bisphenolate ligands exceeded that the mononuclear Ti complex displayed in Figure 2. These aforementioned findings inspired us to design the dinuclear Ti complexes bearing hydrazine-bridging Schiff base ligands with bridging isopropoxide groups, which may improve the catalytic activity of Ti complexes bearing Schiff base ligands. In this study, a series of the hydrazine-bridging Schiff base ligands

and associated Ti complexes were synthesized, and their application in *L*-LA polymerization was studied.

2.0. RESULTS AND DISCUSSION

2.1. Synthesis and Characterization of Ti Complexes.

Symmetrical hydrazine-bridging Schiff base ligands were synthesized by condensing the derivatives of 2-hydroxyphenone or 2-hydroxybenzaldehyde with half the equivalent of hydrazine hydrate in ethanol, as illustrated in Scheme 1(A). The unsymmetrical $L^{Cl-H}-H$ was synthesized in two steps, as displayed in Scheme 1(B): (1) Condensation of 4-chlorobenzaldehyde with one equivalent of hydrazine hydrate in ethanol afforded the intermediate 4-chlorobenzylidenehydrazide; (2) one equivalent of salicylaldehyde was reacted with 4-chlorobenzylidenehydrazide to provide $L^{Cl-H}-H$ with reasonable yields. All the symmetrical ligands reacted with two equivalent of Ti isopropoxide in toluene to obtain a moderate yield of Ti compounds (Scheme 1(A)). The crystal of $L^{CH_3}-Ti_2O(OPr)_2$ was observed from $L^{CH_3}-Ti(OPr)_6$ in the nuclear magnetic resonance (NMR) tube in the air after 2 weeks. The reaction of $L^{CH_3}-Ti_2O(OPr)_2$ synthesis may have comprised the disproportionation product of $L^{CH_3}-Ti(OPr)_6$ reacting with H_2O to replace isopropoxide. $L^{Cl-H}-TiOPr_2$ was synthesized from the reaction of $L^{Cl-H}-H$ and Ti isopropoxide (1:1). The reaction of one equivalent of $L^{Cl-H}-H$ and two

Received: November 9, 2015

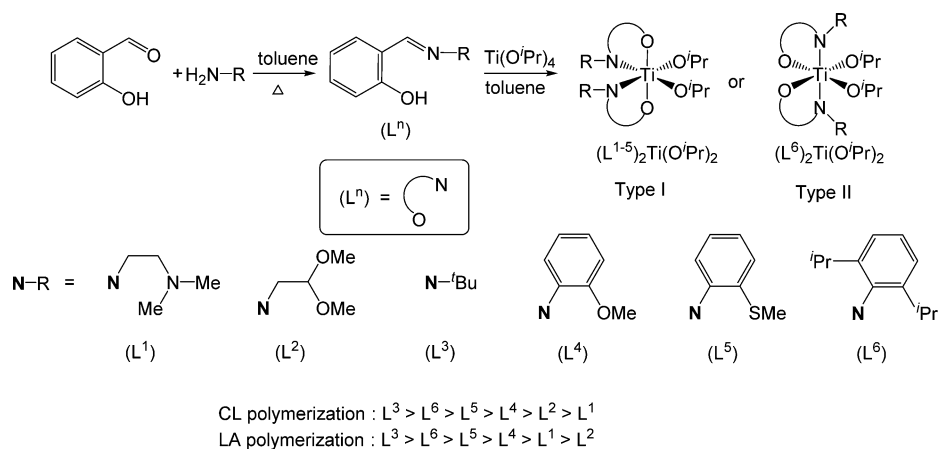


Figure 1. Structures and their catalytic activity of Ti complexes bearing Schiff base ligands.

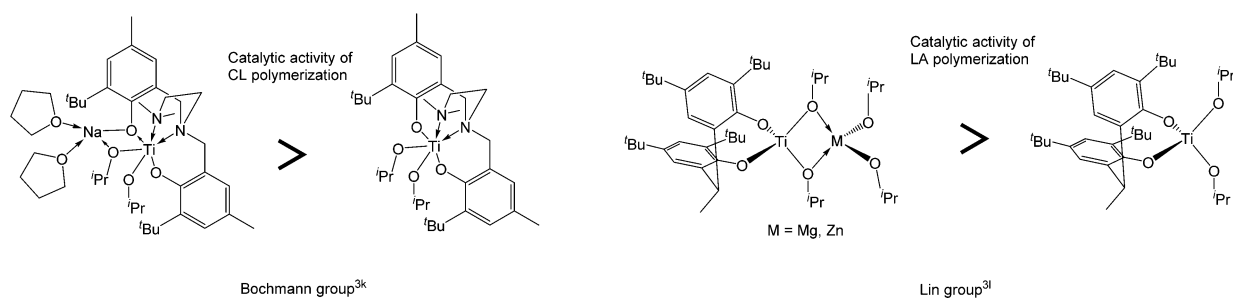
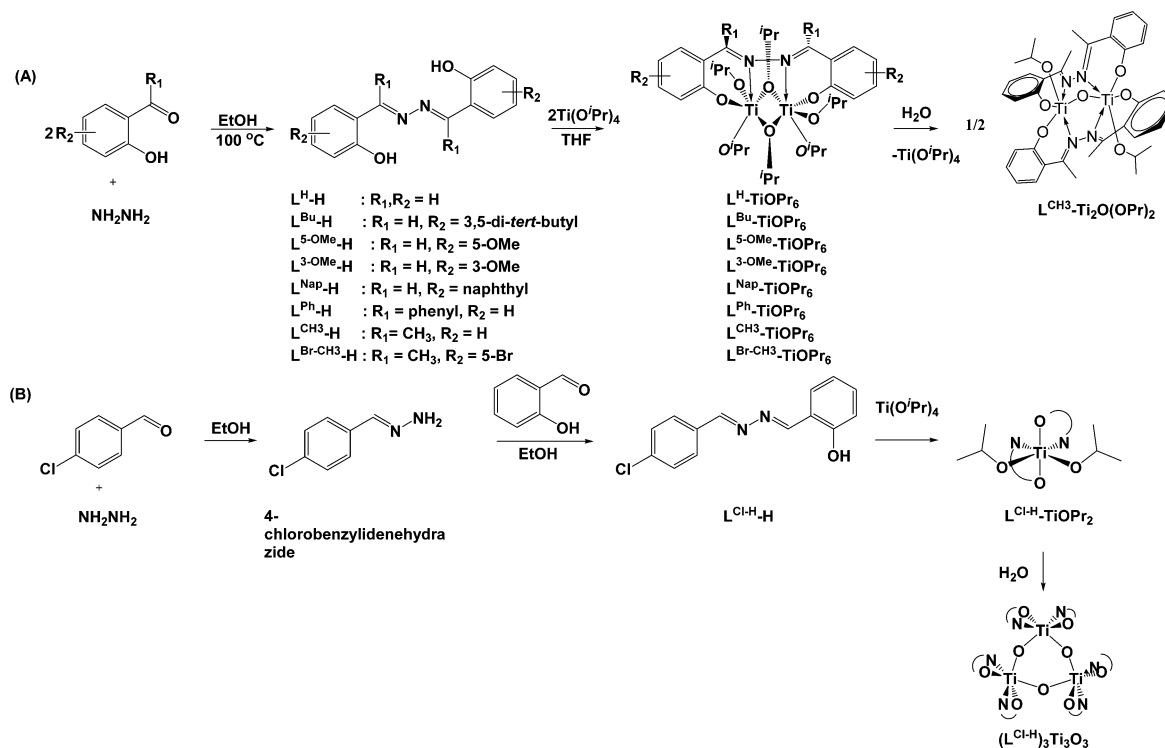


Figure 2. Comparison of catalytic activity between heterobimetallic and mononuclear Ti complexes.

Scheme 1. Synthesis of Hydrazine-Bridging Schiff Base Ligands and Associated Ti Complexes



equivalents of Ti isopropoxide was also attempted; however, only $L^{Cl-H}-TiOPr_2$ was observed. $((L^{Cl-H})_3Ti_3O_3)$ was synthesized from the reaction of $L^{Cl-H}-TiOPr_2$ and H_2O in THF.

The X-ray structure of $L^{Bu}-TiOPr_6$ (Figure 3) reveals the disordered octahedral geometry of the dinuclear Ti complex with

four terminal isopropoxide groups and two bridging isopropoxide groups. $L^{Bu}-TiOPr_6$ possesses C_2 symmetry with a C_2 axis through the center between $N(2)-N(1)$ and $Ti(2)-Ti(1)$ and perpendicular to the lines of $N(2)-N(1)$ and $Ti(2)-Ti(1)$. The angle between $C(15)-N(1)-Ti(1)$ and $C(16)-N(2)-Ti(2)$

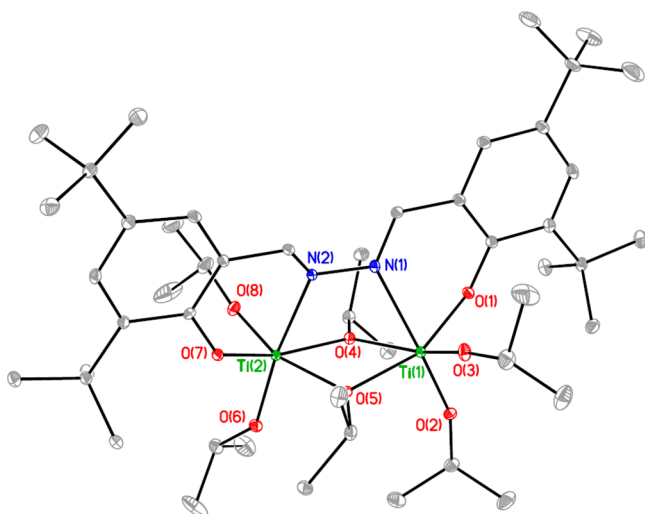


Figure 3. Molecular structure of $L^{\text{Bu}}\text{-TiOPr}_6$ as 20% probability ellipsoids (all of the hydrogen atoms were omitted for clarity). Selected bond lengths (Å) and bond angles (deg): Ti(1)–O(2) 1.7812(18), Ti(1)–O(3) 1.7830(19), Ti(1)–O(1) 1.9347(16), Ti(1)–O(5) 2.0144(15), Ti(1)–O(4) 2.0905(17), Ti(1)–N(1) 2.264(2), Ti(1)–Ti(2) 3.2415(6), Ti(2)–O(7) 1.7885(17), Ti(2)–O(6) 1.8055(18), Ti(2)–O(8) 1.9193(16), Ti(2)–O(4) 2.0028(15), Ti(2)–O(5) 2.0600(16), Ti(2)–N(2) 2.316(2), O(2)–Ti(1)–O(3) 102.62(9), O(2)–Ti(1)–O(1) 96.71(7), O(3)–Ti(1)–O(1) 94.63(8), O(2)–Ti(1)–O(5) 99.94(7), O(3)–Ti(1)–O(5) 93.62(7), O(1)–Ti(1)–O(5) 159.32(7), O(2)–Ti(1)–O(4) 96.59(8), O(3)–Ti(1)–O(4) 157.98(7), O(1)–Ti(1)–O(4) 93.69(7), O(5)–Ti(1)–O(4) 72.35(6), O(2)–Ti(1)–N(1) 170.05(8), O(3)–Ti(1)–N(1) 86.96(8), O(1)–Ti(1)–N(1) 79.65(7), O(5)–Ti(1)–N(1) 81.89(7), O(4)–Ti(1)–N(1) 74.54(7), O(2)–Ti(1)–Ti(2) 109.73(6), O(3)–Ti(1)–Ti(2) 124.25(6), O(1)–Ti(1)–Ti(2) 124.01(5), O(5)–Ti(1)–Ti(2) 37.78(5), O(4)–Ti(1)–Ti(2) 36.70(4), N(1)–Ti(1)–Ti(2) 65.86(5), O(7)–Ti(2)–O(6) 99.67(9), O(7)–Ti(2)–O(8) 94.64(8), O(6)–Ti(2)–O(8) 97.72(8), O(7)–Ti(2)–O(4) 92.77(7), O(6)–Ti(2)–O(4) 101.13(7), O(8)–Ti(2)–O(4) 158.26(8), O(7)–Ti(2)–O(5) 162.50(7), O(6)–Ti(2)–O(5) 93.45(7), O(8)–Ti(2)–O(5) 95.02(7), O(4)–Ti(2)–O(5) 73.23(6), O(7)–Ti(2)–N(2) 93.05(8), O(6)–Ti(2)–N(2) 166.91(8), O(8)–Ti(2)–N(2) 78.03(7), O(4)–Ti(2)–N(2) 81.20(7), O(5)–Ti(2)–N(2) 74.77(7).

planes is 38.33° . The X-ray structure of $L^{\text{CH}_3}\text{-Ti}_2\text{O(OPr)}_2$ (Figure 4) also displays the disordered octahedral geometry of the dinuclear Ti complex with two terminal isopropoxide groups and one bridging oxide. $L^{\text{CH}_3}\text{-Ti}_2\text{O(OPr)}_2$ possesses C_2 symmetry with a C_2 axis through the oxide and perpendicular to the lines of N(2)–N(4), N(1)–N(3), and Ti(2)–Ti(1). $L^{\text{Cl-H}}\text{-TiOPr}_2$ (Figure 5) reveals a common type I (Figure 1, cis for N–N) Ti complex in the octahedral form with two terminal isopropoxide groups and two $L^{\text{Cl-H}}\text{-O}^-$ ligands, which exhibits no coordination of N atoms in the 4-chlorobenzylidene group. The geometry of Ti atoms in $(L^{\text{Cl-H}})_3\text{Ti}_3\text{OPr}_3$ (Figure 6) is similar to that in $L^{\text{Cl-H}}\text{-TiOPr}_2$, except that two terminal isopropoxide groups are placed with one oxide and a six-membered ring, and a trinuclear form with D_3 symmetry is constructed with three Ti–O units.

2.2. Polymerization of Lactides. LA polymerization using Ti complexes as initiators in toluene was investigated under nitrogen at 60°C (Table 1). As exhibited in entries 1, 5, and 6 of Table 1, Ti complexes with ligands, where R^1 were H, methyl (CH_3), and phenyl (ph) groups, exhibited different catalytic activities according to the substitutes in the imino group, and the catalytic trend of R^1 was $\text{H} > \text{CH}_3 > \text{ph}$. $L^{\text{Bu}}\text{-TiOPr}_6$ (entry 2,

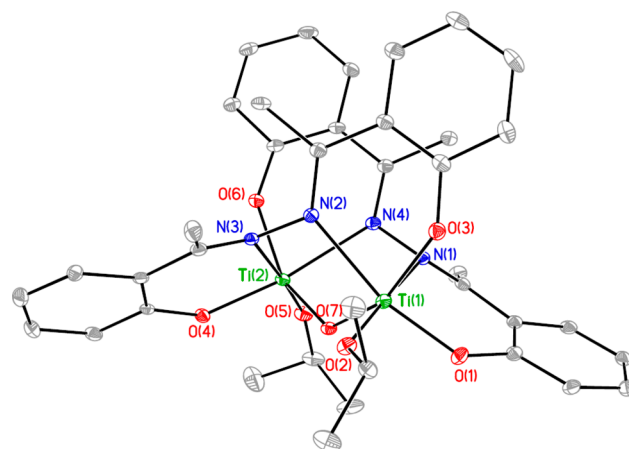


Figure 4. Molecular structure of $L^{\text{CH}_3}\text{-Ti}_2\text{O(OPr)}_2$ as 20% probability ellipsoids (all of the hydrogen atoms were omitted for clarity). Selected bond lengths (Å) and bond angles (deg): Ti(1)–O(2) 1.795(3), Ti(1)–O(7) 1.836(3), Ti(1)–O(1) 1.892(3), Ti(1)–O(3) 1.931(3), Ti(1)–N(2) 2.244(3), Ti(1)–N(1) 2.324(3), Ti(2)–O(5) 1.796(3), Ti(2)–O(7) 1.843(3), Ti(2)–O(4) 1.885(3), Ti(2)–O(6) 1.921(3), Ti(2)–N(3) 2.255(3), Ti(2)–N(4) 2.293(3), O(2)–Ti(1)–O(7) 100.15(13), O(2)–Ti(1)–O(1) 97.90(13), O(7)–Ti(1)–O(1) 103.51(13), O(2)–Ti(1)–O(3) 100.76(13), O(7)–Ti(1)–O(3) 152.10(12), O(1)–Ti(1)–O(3) 91.67(13), O(2)–Ti(1)–N(2) 94.46(13), O(7)–Ti(1)–N(2) 82.16(12), O(1)–Ti(1)–N(2) 165.20(13), O(3)–Ti(1)–N(2) 78.00(12), O(2)–Ti(1)–N(1) 173.54(13), O(7)–Ti(1)–N(1) 74.31(12), O(1)–Ti(1)–N(1) 80.45(12), O(3)–Ti(1)–N(1) 85.56(12), N(2)–Ti(1)–N(1) 88.13(12), O(5)–Ti(2)–O(7) 101.34(13), O(5)–Ti(2)–O(4) 97.26(13), O(7)–Ti(2)–O(4) 101.60(12), O(5)–Ti(2)–O(6) 100.23(14), O(7)–Ti(2)–O(6) 149.61(12), O(4)–Ti(2)–O(6) 96.61(12), O(5)–Ti(2)–N(3) 176.11(13), O(7)–Ti(2)–N(3) 76.52(12), O(4)–Ti(2)–N(3) 80.10(12), O(6)–Ti(2)–N(3) 82.97(12), O(5)–Ti(2)–N(4) 90.42(13), O(7)–Ti(2)–N(4) 81.00(12), O(4)–Ti(2)–N(4) 171.18(12), O(6)–Ti(2)–N(4) 77.68(12), N(3)–Ti(2)–N(4) 92.43(12).

Table 1) illustrated that the steric effect in the phenol group reduced the catalytic activity and $L^{3\text{-OMe}}\text{-TiOPr}_6$, $L^{5\text{-OMe}}\text{-TiOPr}_6$, and $L^{\text{Br-CH}_3}\text{-TiOPr}_6$ (entries 3, 4 and 8, respectively, Table 1) displayed that electron donating groups slightly increased the catalytic activity. In addition, Ti complexes bearing Schiff base ligands with the substitutes in the phenol group, such as $L^{\text{Bu}}\text{-TiOPr}_6$, $L^{5\text{-OMe}}\text{-TiOPr}_6$, $L^{3\text{-OMe}}\text{-TiOPr}_6$, $L^{\text{Nap}}\text{-TiOPr}_6$, and $L^{\text{Br-CH}_3}\text{-TiOPr}_6$, exhibited a low controllability of polymer molecular weight and a broad polydispersity index (PDI). The spectra of ESI-MS (Figure S25) and ^1H NMR (Figure S26) indicated the polymer chain should be capped with one isopropoxide ester and one hydroxy end, suggesting that back reactions leading to the formation of macrocycles do not occur. Furthermore, the catalytic activity of all dinuclear Ti complexes bearing hydrazine-bridging Schiff base ligands was higher (approximately 10–60-fold) than that of mononuclear $L^{\text{Cl-H}}\text{-TiOPr}_2$, implying that the strategy of bridging dinuclear Ti complexes with isopropoxide groups in the ROP of LA was successful. On the basis of the linear relationship between Mn_{GPC} and $([\text{LA}]_0 \times \text{conv.})/[\text{L}^{\text{H}}\text{-TiOPr}_6]$ exhibited in Figure 7, polymerizing LA by using $L^{\text{H}}\text{-TiOPr}_6$ as the catalyst demonstrated high controllability with a narrow PDI. However, Figure 7 reveals that only four isopropoxides groups in $L^{\text{H}}\text{-TiOPr}_6$ were initiators during the polymerization process. In addition, *rac*-LA polymerization using these Ti complexes as initiators was also investigated and shown in Table S3. However, the results of the

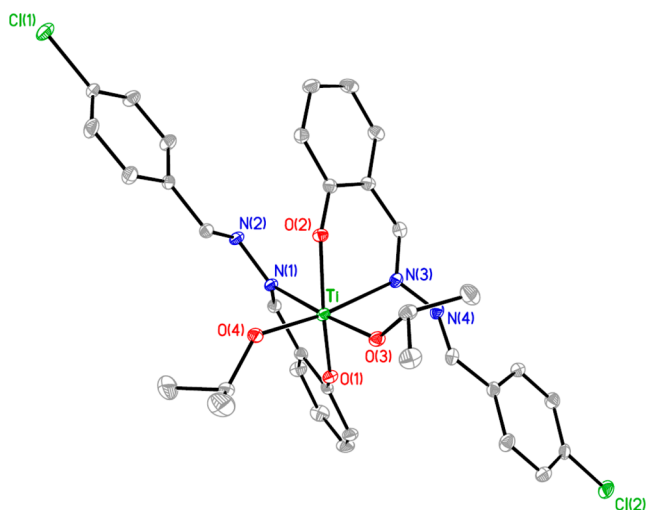


Figure 5. Molecular structure of $L^{Cl-H}\text{-TiOPr}_2$, as 30% probability ellipsoids (all of the hydrogen atoms were omitted for clarity). Selected bond lengths (Å) and bond angles (deg): Ti–O(3) 1.8164(13), Ti–O(4) 1.8221(14), Ti–O(2) 1.8898(15), Ti–O(1) 1.8962(14), Ti–N(3) 2.3398(17), Ti–N(1) 2.3491(16), O(3)–Ti–O(4) 100.51(6), O(3)–Ti–O(2) 98.85(6), O(4)–Ti–O(2) 96.46(6), O(3)–Ti–O(1) 96.57(6), O(4)–Ti–O(1) 98.15(6), O(2)–Ti–O(1) 156.41(6), O(3)–Ti–N(3) 89.06(6), O(4)–Ti–N(3) 170.15(6), O(2)–Ti–N(3) 79.64(6), O(1)–Ti–N(3) 82.89(6), O(3)–Ti–N(1) 170.99(6), O(4)–Ti–N(1) 88.14(6), O(2)–Ti–N(1) 82.50(6), O(1)–Ti–N(1) 79.58(6), N(3)–Ti–N(1) 82.40(6).

selectivity of poly-*rac*-LA were not special ($P_r(L^{Nap}) = 52\%$, $P_r(L^H) = 38\%$, $P_r(L^{5-OMe}) = 44\%$, $P_r(L^{Ph}) = 54\%$, $P_r(L^{Br-CH_3}) = 50\%$, $P_r(L^{Bu}) = 51\%$).

2.3. Kinetic Studies of LA Polymerization Catalyzed by $L^H\text{-TiOPr}_6$. Kinetic studies were performed at 60 °C with respect to the ratio of $[LA]_0/[L^H\text{-TiOPr}_6]$ ($[LA] = 2.5$ M in 5 mL of toluene) as exhibited in Table S2 and Figures 8 and 9. The preliminary results indicated a first-order dependency on $[LA]$ (Figure 8). By plotting k_{obs} against $[L^H\text{-TiOPr}_6]$, a k_{prop} value of 4.03 ($M^{-1}min^{-1}$) was obtained (Figure 9). Polymerizing LA by using $L^H\text{-TiOPr}_6$ at 60 °C demonstrated the following rate law:

$$d[LA]/dt = 4.03 \times [LA][L^H\text{-TiOPr}_6]$$

2.4. Mechanistic Studies of Polymerization. The polymerization data revealed that only four isopropoxide groups in Ti complexes were initiators during polymerization. To realize the role of these six isopropoxide groups, the 1H NMR spectra of the mixture of one equivalent of $L^{CH_3}\text{-TiOPr}_6$ and six equivalents of LA in $CDCl_3$ at 60 °C were studied, as displayed in Figures 10 and S2. Figure 10 reveals that the isopropoxide groups began initiating LA at 40 °C, but the initiation rate was extremely slow. After 2 days at 60 °C, the polymerization rate for isopropoxide groups a and b decreased evidently, but the isopropoxide group c still existed. Thus, only four terminal isopropoxide groups could initiate LA polymerization; this is consistent with the polymerization results. This phenomenon was similar to the polymerization achieved by using other dinuclear Ti complexes^{3m} as catalysts.

According to the polymerization results, kinetic characteristics, and 1H NMR study, one monomer was consumed in every polymerization cycle, and the Ti complexes retained the dinuclear form because the order of the monomer and Ti complex was 1. The possible polymerization mechanism is provided in Figure 11. One of the bridging isopropoxide groups increased the bond with

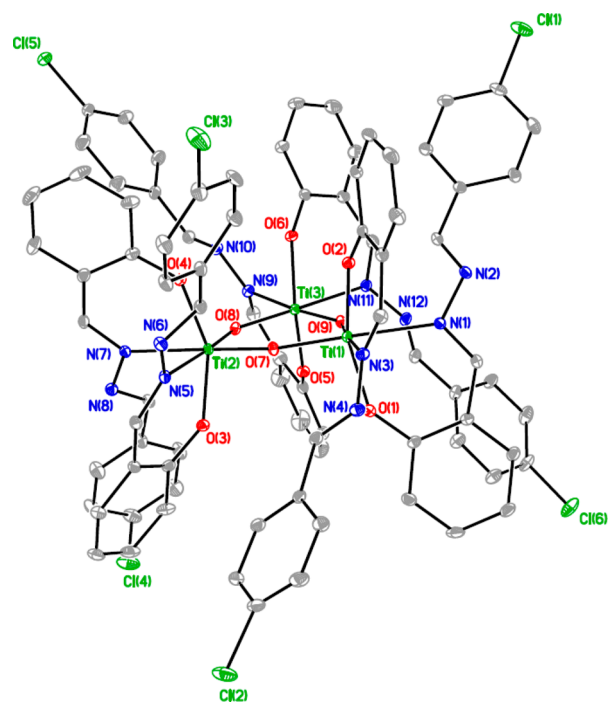


Figure 6. Molecular structure of $(L^{Cl-H})_3Ti_3OPr_3$ as 20% probability ellipsoids (all of the hydrogen atoms were omitted for clarity). Selected bond lengths (Å) and bond angles (deg): Ti(1)–O(9) 1.8043(16), Ti(1)–O(7) 1.8353(16), Ti(1)–O(2) 1.8942(17), Ti(1)–O(1) 1.8961(18), Ti(1)–N(1) 2.3072(19), Ti(1)–N(3) 2.327(2), Ti(2)–O(7) 1.8113(16), Ti(2)–O(8) 1.8351(17), Ti(2)–O(3) 1.9021(18), Ti(2)–O(4) 1.9023(17), Ti(2)–N(5) 2.322(2), Ti(2)–N(7) 2.324(2), Ti(3)–O(8) 1.8173(16), Ti(3)–O(9) 1.8236(16), Ti(3)–O(6) 1.8927(18), Ti(3)–O(5) 1.9031(17), Ti(3)–N(9) 2.293(2), Ti(3)–N(11) 2.318(2), O(9)–Ti(1)–O(7) 95.35(7), O(9)–Ti(1)–O(2) 98.69(8), O(7)–Ti(1)–O(2) 96.48(7), O(9)–Ti(1)–O(1) 98.09(8), O(7)–Ti(1)–O(1) 98.19(8), O(2)–Ti(1)–O(1) 156.52(7), O(9)–Ti(1)–N(1) 87.09(7), O(7)–Ti(1)–N(1) 177.46(7), O(2)–Ti(1)–N(1) 83.82(7), O(1)–Ti(1)–N(1) 80.75(7), O(9)–Ti(1)–N(3) 175.83(7), O(7)–Ti(1)–N(3) 88.62(7), O(2)–Ti(1)–N(3) 79.54(7), O(1)–Ti(1)–N(3) 82.58(7), N(1)–Ti(1)–N(3) 88.96(7), O(7)–Ti(2)–O(8) 96.25(7), O(7)–Ti(2)–O(3) 98.07(8), O(8)–Ti(2)–O(3) 100.36(8), O(7)–Ti(2)–O(4) 99.90(8), O(8)–Ti(2)–O(4) 96.67(8), O(3)–Ti(2)–O(4) 153.65(7), O(7)–Ti(2)–N(5) 88.06(7), O(8)–Ti(2)–N(5) 175.66(7), O(3)–Ti(2)–N(5) 79.55(7), O(4)–Ti(2)–N(5) 81.96(7), O(7)–Ti(2)–N(7) 176.81(7), O(8)–Ti(2)–N(7) 86.94(7), O(3)–Ti(2)–N(7) 81.27(7), O(4)–Ti(2)–N(7) 79.71(7), N(5)–Ti(2)–N(7) 88.75(7), O(8)–Ti(3)–O(9) 96.00(7), O(8)–Ti(3)–O(6) 99.93(8), O(9)–Ti(3)–O(6) 96.59(8), O(8)–Ti(3)–O(5) 96.99(8), O(9)–Ti(3)–O(5) 99.74(7), O(6)–Ti(3)–O(5) 155.04(8), O(8)–Ti(3)–N(9) 90.75(7), O(9)–Ti(3)–N(9) 173.20(7), O(6)–Ti(3)–N(9) 81.45(8), O(5)–Ti(3)–N(9) 80.11(8), O(8)–Ti(3)–N(11) 177.88(7), O(9)–Ti(3)–N(11) 86.11(7), O(6)–Ti(3)–N(11) 79.96(8), O(5)–Ti(3)–N(11) 82.45(8), N(9)–Ti(3)–N(11) 87.14(7).

the Ti atom on the left side and reduced the bond with the Ti atom on the right side to increase the space around the Ti atom on the right side. LA bonded to the Ti atom to form a hepta-coordinated form (transition state A in Figure 11). The crowded hepta-coordinated transition state enhanced the initiation of terminal isopropoxide to LA, thereby releasing unstable energy as well as continually repeating the coordination of monomers and the initiation of alkoxide to produce the polymer. $L^{Cl-H}\text{-TiOPr}_2$ exhibited low activity because coordinating the monomer was

Table 1. Polymerizing L-Lactide by Using Each of the Ti Complexes as an Initiator at 60 °C^d

Entry	L-TiOPr ₆ , L=	Time (min)	Conv. ^a	Mn _{Cal} ^b	Mn _{GPC} ^c	PDI ^c	k _{obs} (10 ⁻³ min ⁻¹)
1	L ^H	50	89%	2200	3100	1.25	65.21 (298)
2	L ^{Bu}	110	91%	2200	2400	1.39	33.64 (162)
3	L ^{5-OMe}	50	93%	2200	4100	1.82	70.09 (227)
4	L ^{3-OMe}	30	92%	2200	4000	1.94	94.20 (513)
5	L ^{Nap}	80	99%	2500	4300	1.86	63.31 (157)
6	L ^{Ph}	240	96%	2400	4000	1.10	12.57 (49)
7	L ^{CH3}	150	99%	2500	7800	1.34	25.57 (201)
8	L ^{Br-CH3}	300	99%	2500	5600	1.93	14.17 (82)
9 ^e	L ^{Cl-H} -TiOPr ₂	3000	99%	3600	2500	1.10	1.18 (9)
10 ^f	L ^H	60	93%	4500	6100	1.31	
11 ^g	L ^H	60	87%	2800	3500	1.24	
12 ^h	L ^H	60	89%	1000	1600	1.09	
13 ⁱ	L ^H	180	93%	11200	18500	1.29	

^aObtained from ¹H NMR analysis. ^bCalculated from the molecular weight of monomer × [monomer]₀/[ⁱPrO⁻]₀ × conversion yield + Mw(PrⁱO). ^cObtained from GPC analysis and calibration based on the polystyrene standard. Values of Mn_{GPC} are the values obtained from GPC times 0.58. ^dReaction condition: toluene (5 mL), [LA] = 2.0 M, [LA]:[Cat] = 100:1. ^eReaction condition: toluene (5 mL), [LA] = 2.0 M, [LA]:[Cat] = 100:2. ^fReaction condition: toluene (5 mL), [LA] = 2.0 M, [LA]:[Cat] = 100:0.5. ^gReaction condition: toluene (5 mL), [LA] = 2.0 M, [LA]:[Cat] = 100:0.75. ^hReaction condition: toluene (5 mL), [LA] = 2.0 M, [LA]:[Cat] = 100:2. ⁱReaction condition: toluene (5 mL), [LA] = 2.0 M, [LA]:[Cat] = 100:0.2.

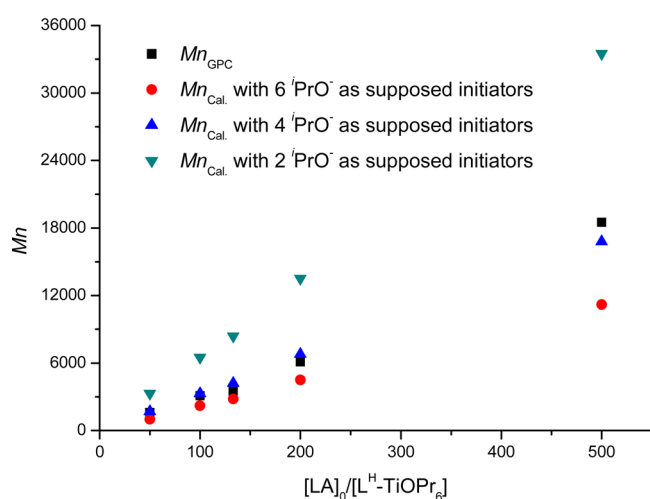


Figure 7. Linear plot of various Mn_{cal.} with the supposed initiators and Mn_{GPC} against [LA]₀ × conv./[L^H-TiOPr₆] (Table 1, entries 1 and 10–13).

difficult without the adjusting of the bridging isopropoxide group to the stable hepta-coordinated form. In addition, the hydrazine-bridging Schiff base ligands added more space around the Ti atom than the other dinuclear Ti complex^{3m} displayed in Figure 12 did. Figure 12 reveals that the distance of between the two oxygen atoms of the terminal isopropoxide groups, which were in the trans-position to the imine groups of L^{Bu}-TiOPr₆, was 4.429 Å and longer than that of the other dinuclear Ti complex^{3m} (3.947 Å). This result demonstrated that LA coordination in Ti complexes bearing hydrazine-bridging Schiff base ligands was easier and the catalytic activity was higher (L^H-TiOPr₆: conv. = 93% in 180 min, [Cat] = 4.0 mM, [LA]:[Cat] = 500:1 at 60 °C; other dinuclear Ti complex:^{3m} conv. = 89% in 12 h, [Cat] = 4.0 mM, [LA]:[Cat] = 500:1 at 100 °C). To explain the difference of the catalytic rates of L^{Ph}-TiOPr₆, L^{CH3}-TiOPr₆, and L^H-TiOPr₆, the density functional theory (DFT) calculation of two dinuclear forms of L^{Bu-Ph}-TiOPr₆ and L^{Bu-CH3}-TiOPr₆ (Figure 13) was studied, and the data were compared with L^{Bu}-TiOPr₆. Figure 13 reveals that the distance between two

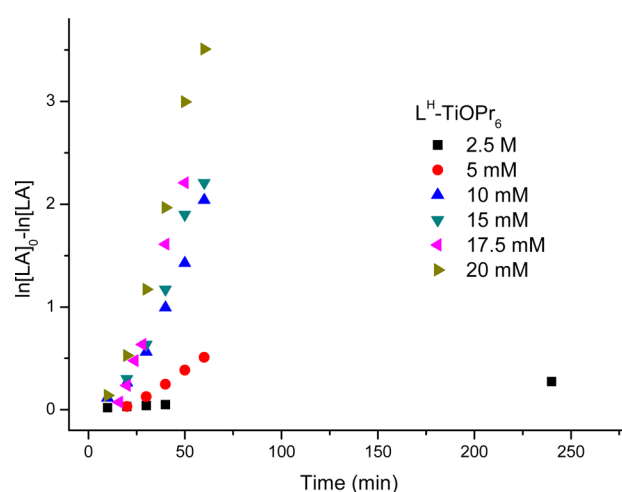


Figure 8. First-order kinetic plots of LA polymerization with various concentrations of [L^H-TiOPr₆] plotted against time with [LA] = 2.5 M in toluene (5 mL).

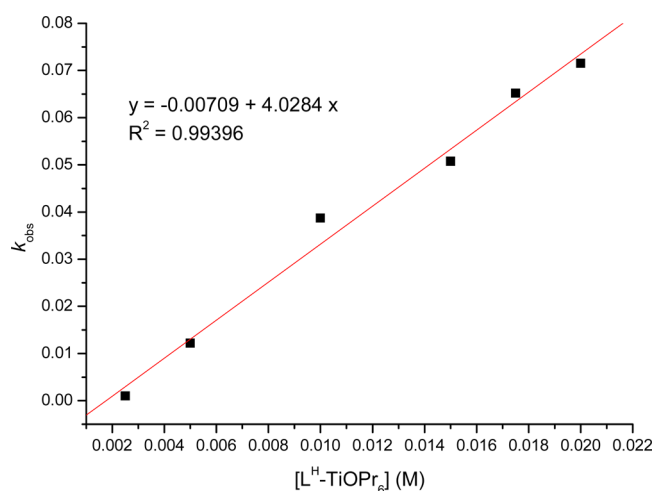


Figure 9. Linear plot of k_{obs} against [L^H-TiOPr₆] for LA polymerization with [LA] = 2.5 M in toluene (5 mL).

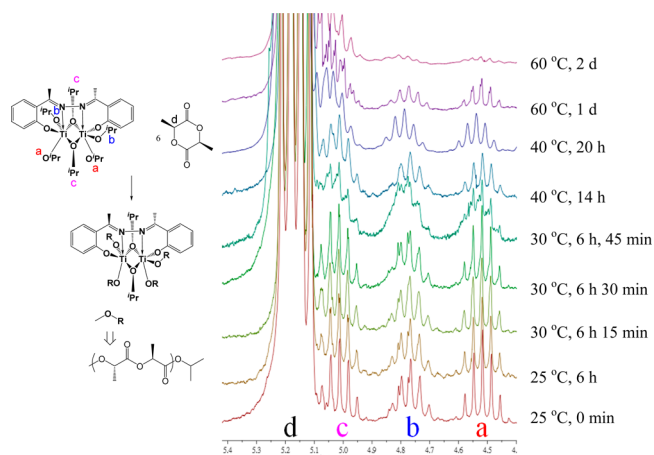


Figure 10. ^1H NMR study of the mixture of one equivalent of $\text{L}^{\text{CH}_3}\text{-TiOPr}_6$ and six equivalents of LA in CDCl_3 at $60\text{ }^\circ\text{C}$.

oxygen atoms of the terminal isopropoxide groups, which were in the trans-position to the imine groups of $\text{L}^{\text{Bu}}\text{-TiOPr}_6$, exceeded that of $\text{L}^{\text{Bu-CH}_3}\text{-TiOPr}_6$ (4.385 Å) and $\text{L}^{\text{Bu-Ph}}\text{-TiOPr}_6$ (4.300 Å) because of the steric effect between the substituent on the imine groups. Moreover, compared with $\text{L}^{\text{Ph}}\text{-TiOPr}_6$ and $\text{L}^{\text{CH}_3}\text{-TiOPr}_6$, $\text{L}^{\text{H}}\text{-TiOPr}_6$ with more space around the Ti atom displayed highest catalytic activity.

3.0. CONCLUSIONS

This study synthesized a series of hydrazine-bridging Schiff base ligands and their corresponding titanium complexes. The electronic and steric effects of the phenolate group altered LA polymerization. If the ligands of Ti complexes were electron withdrawing or steric bulky groups, then the degree of activity would decrease dramatically. In addition, the steric bulky substituent on the imine groups reduced the space around the Ti atom and then reduced LA coordination with Ti atom contents, thereby reducing catalytic activity. The catalytic activities of all dinuclear Ti complexes exceeded (approximately 10–60-fold)

that of mononuclear $\text{L}^{\text{Cl-H}}\text{-TiOPr}_2$. Overall, the strategy of bridging dinuclear Ti complexes with isopropoxide groups in the ROP of LA was successful, and the adjustment of the crowded heptacoordinated transition state by the bridging isopropoxides may explain the success of our strategy.

4.0. EXPERIMENTAL SECTION

Standard Schlenk techniques and a N_2 -filled glovebox were used all over the isolation and treatment of all the compounds. Solvents, *L*-lactide, and deuterated solvents were purified prior to use. Salicylaldehyde, 2-hydroxy-5-methoxybenzaldehyde, 3,5-di-*tert*-butyl-2-hydroxybenzaldehyde, 1-(5-bromo-2-hydroxyphenyl)ethan-1-one, 1-(2-hydroxyphenyl)ethan-1-one, 4-chlorobenzaldehyde, 3-hydroxy-2-naphthaldehyde, hydrazine monohydrate and benzyl alcohol were purchased from Aldrich. ^1H and ^{13}C NMR spectra were recorded on a Varian Gemini2000–200 (200 MHz for ^1H and 50 MHz for ^{13}C) spectrometer with chemical shifts given in ppm from the internal TMS or center line of CDCl_3 . Microanalyses were performed using a Heraeus CHN-O-RAPID instrument. The gel permeation chromatography (GPC) measurements were performed on a Waters 1515 Isocratic HPLC pump system equipped with a differential Waters 2414 refractive index detector using THF (HPLC grade) as the eluent. The chromatographic column was a Water Styragel Column (HR4E), and the calibration curve was made by polystyrene standards to calculate Mn (GPC). Ligands of $\text{L}^{\text{H}}\text{-H}$,⁴ $\text{L}^{\text{nap}}\text{-H}$,⁵ $\text{L}^{\text{CH}_3}\text{-H}$,⁶ $\text{L}^{\text{Bu}}\text{-H}$,⁷ and $\text{L}^{\text{Ph}}\text{-H}$ ⁸ were prepared by acid-catalyzed condensation following literature procedures. DFT geometry optimizations were carried out at M06/6-31G* level combined with the D3 version of Grimme's dispersion correction. Calculations were performed by Gaussian 09 program.

Synthesis of $\text{L}^{3\text{-OMe}}\text{-H}$. Hydrazine monohydrate (1.16 g, 23.0 mmol) was added dropwise into an ethanol solution (100 mL) of the 2-hydroxy-3-methoxybenzaldehyde (7.1 g, 46.6 mmol) at room temperature. The resulting solution was refluxed for 1 day. The product precipitated as a yellow solid which was filtered. Yield: 5.18 g (69%). ^1H NMR (CDCl_3 , 200 MHz): δ 10.99 (1H, s, OH), 8.68 (2H, s, $\text{CH}=\text{N}$), 7.04–6.96 (4H, m, ArH), 6.85 (1H, s, ArH), 3.81 (6H, s, OCH_3). ^{13}C NMR spectrum was not available because of low solubility of $\text{L}^{\text{OMe}}\text{-H}$ in CDCl_3 . Mp = 188 $^\circ\text{C}$

Synthesis of $\text{L}^{5\text{-OMe}}\text{-H}$. Using a method similar to that for $\text{L}^{3\text{-OMe}}\text{-H}$ expect 1-(5-methoxy-2-hydroxyphenyl)ethan-1-one was used in place of 2-hydroxy-3-methoxybenzaldehyde. Yield: 5.25 g (75%). ^1H NMR (CDCl_3 , 200 MHz): δ 10.99 (1H, s, OH), 8.68 (2H, s, $\text{CH}=\text{N}$),

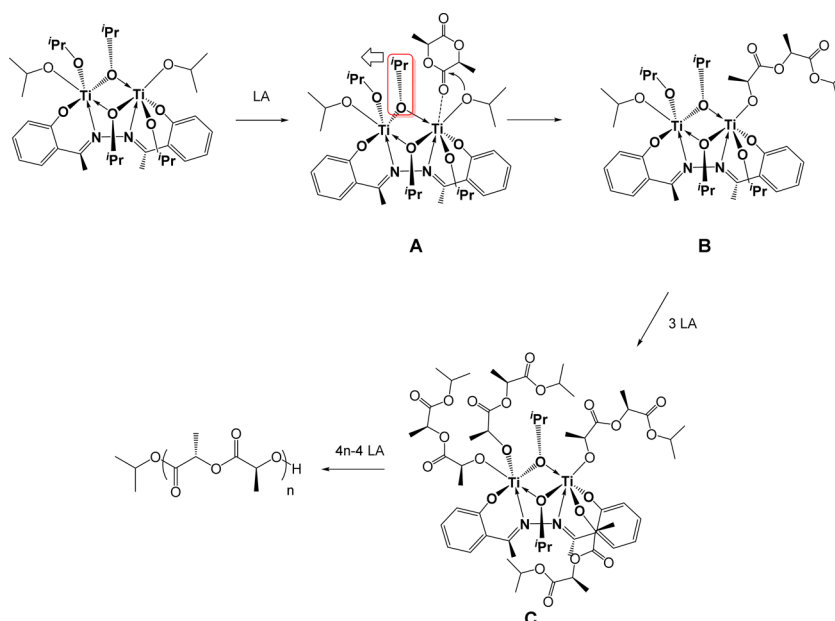


Figure 11. Possible mechanism of polymerization using Ti complexes bearing hydrazine-bridging Schiff base ligands as catalysts.

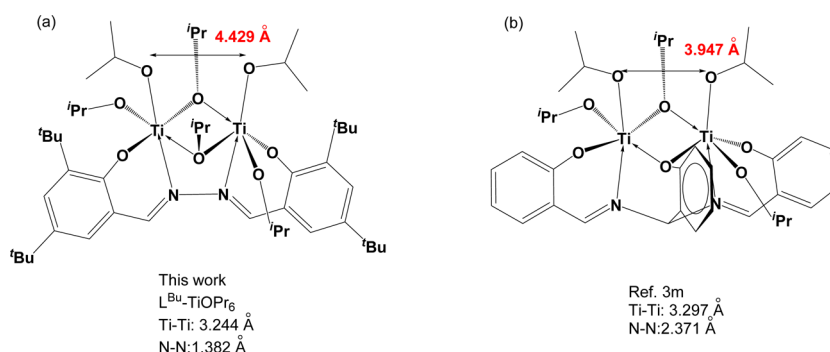


Figure 12. Structural comparison of dinuclear Ti complexes bearing (a) hydrazine-bridging Schiff base ligands and (b) *N,N*-di(salicylidene)-2-hydroxyphenylmethanediamine.^{3m}

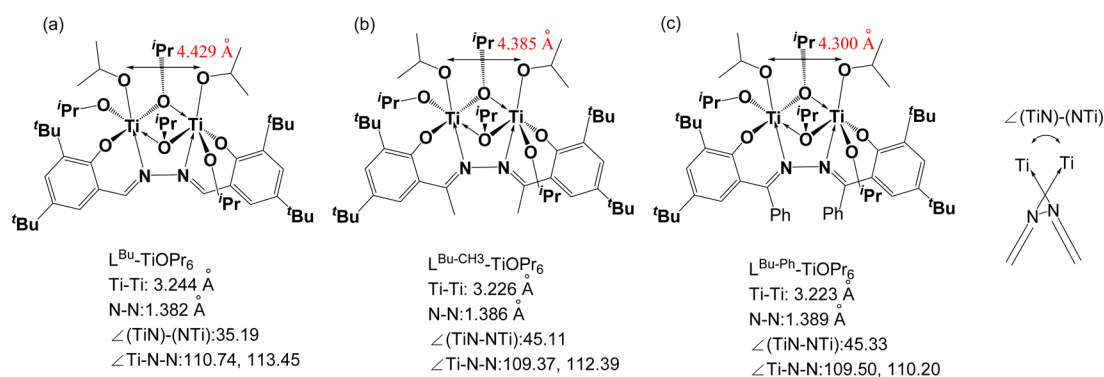


Figure 13. Structural comparison of dinuclear Ti complexes bearing (a) $L^{\text{Bu}}\text{-TiOPr}_6$, (b) $L^{\text{CH}_3}\text{-TiOPr}_6$, and (c) $L^{\text{Ph}}\text{-TiOPr}_6$.

7.04–6.96 (4H, m, ArH), 6.85 (1H, s, ArH), 3.81 (6H, s, OCH₃). ¹³C NMR spectrum was not available because of low solubility of $L^{\text{OMe}}\text{-H}$ in CDCl₃. Mp = 210 °C

Synthesis of $L^{\text{Br-CH}_3}\text{-H}$. Using a method similar to that for $L^{\text{3-OMe}}\text{-H}$ expect 1-(5-bromo-2-hydroxyphenyl)ethan-1-one was used in place of 2-hydroxy-3-methoxybenzaldehyde. Yield: 10.227 g (48%). ¹H NMR (CDCl₃, 200 MHz): δ 7.74 (2H, s, ArH), 7.47, 6.94 (4H, d, *J* = 10 Hz, ArH), 2.55 (6H, s, N=CCH₃). ¹³C NMR spectrum was not available because of low solubility of $L^{\text{Br-CH}_3}\text{-H}$ in CDCl₃. Mp = 292 °C

Synthesis of $L^{\text{Cl-H}}\text{-H}$. 4-chlorobenzaldehyde (7.03 g, 50 mmol) was added dropwise into an ethanol solution (100 mL) of the hydrazine monohydrate (5.0 g, 0.10 mol) at 0 °C for 6 h. Volatile materials were removed under vacuum to give a white powder. 6.625 g of the white powder was reacted with 2-hydroxybenzaldehyde (5.24 g, 43 mmol) in ethanol (50 mL) and refluxed for 1 day. The product precipitated as a yellow solid which was filtered. Yield: 7.12 g (64%). ¹H NMR (CDCl₃, 200 MHz): δ 8.77, 8.59 (2H, s, CH=N), 7.79, 7.45 (4H, d, *J* = 8 Hz, ArH), 7.38–7.34 (2H, m, ArH), 7.05–6.92 (2H, m, ArH). ¹³C NMR spectrum was not available because of low solubility of $L^{\text{Cl-H}}\text{-H}$ in CDCl₃. Mp = 112 °C

Synthesis of $L^{\text{H}}\text{-TiOPr}_6$. A mixture of $L^{\text{H}}\text{-H}$ (1.20 g, 5 mmol) and Ti(O^{*i*}Pr)₄ (2.843 g, 10 mmol) in THF (30 mL), was stirred for 12 h. Volatile materials were removed under vacuum to give yellow oil and then it was washed with hexane (50 mL). The product precipitated as a yellow powder which was filtered. Yield: 2.48 g (72%). ¹H NMR (CDCl₃, 200 MHz): δ 7.94 (2H, s, CH=N), 7.36 (2H, t, *J* = 6 Hz, Ar-H), 7.26 (2H, d, *J* = 6 Hz, Ar-H), 6.82 (2H, d, *J* = 6 Hz, Ar-H), 6.74 (2H, t, *J* = 6 Hz, Ar-H), 4.99, 4.77, 4.48 (sept, 6H, *J* = 5.8 Hz, OCH(CH₃)₂), 1.40–1.12, (m, 24 H, OCH(CH₃)₂), 0.92, 0.89 (d, 12H, *J* = 5.8 Hz, OCH(CH₃)₂). ¹³C NMR (CDCl₃, 50 MHz): δ 165.15 (C=N), 150.93, 134.07, 131.72, 119.97, 119.52, 116.89 (Ar), 78.56, 77.77, 74.68 (OCH(CH₃)₂), 25.91, 25.85, 25.35, 25.13, 24.18, 23.59 (OCH(CH₃)₂). Anal. Calcd (found) for C₃₂H₅₂N₂O₈Ti₂: C, 55.82 (55.45); H, 7.61 (7.62); N, 4.07 (4.67)%. Mp = 122 °C.

Synthesis of $L^{\text{3-OMe}}\text{-TiOPr}_6$. Using a method similar to that for $L^{\text{H}}\text{-TiOPr}_6$ expect $L^{\text{3-OMe}}\text{-H}$ was used in place of $L^{\text{H}}\text{-H}$. Yield: 2.85 g

(76%). ¹H NMR (CDCl₃, 200 MHz): δ 7.94 (2H, s, CH=N), 7.00 (2H, d, *J* = 10 Hz, Ar-H), 6.93 (2H, d, *J* = 7 Hz, Ar-H), 6.66 (2H, t, *J* = 7 Hz, Ar-H), 5.02, 4.78, 4.46 (sept, 6H, *J* = 6.0 Hz, OCH(CH₃)₂), 3.92 (6H, s, OCH₃), 1.40–1.18, (m, 24 H, OCH(CH₃)₂), 0.88 (br, 12H, OCH(CH₃)₂). ¹³C NMR (CDCl₃, 50 MHz): δ 159.97 (C=N), 150.64, 150.51, 121.95, 120.17, 119.16, 113.29 (Ar), 78.25, 77.41, 74.51 (OCH(CH₃)₂), 55.59 (OCH₃), 25.88, 25.28, 25.05, 24.05, 23.55 (OCH(CH₃)₂). Anal. Calcd (found) for C₃₄H₅₆N₂O₁₀Ti₂: C, 54.55 (55.05); H, 7.54 (7.49); N, 3.74 (3.76)%. Mp = 122 °C.

Synthesis of $L^{\text{5-OMe}}\text{-TiOPr}_6$. Using a method similar to that for $L^{\text{H}}\text{-TiOPr}_6$ expect $L^{\text{5-OMe}}\text{-H}$ was used in place of $L^{\text{H}}\text{-H}$. Yield: 1.68 g (43%). ¹H NMR (CDCl₃, 200 MHz): δ 7.92 (2H, s, CH=N), 7.00 (2H, d, *J* = 10 Hz, Ar-H), 6.78 (2H, d, *J* = 10 Hz, Ar-H), 6.75 (2H, s, Ar-H), 4.98, 4.77, 4.48 (sept, 6H, *J* = 5.8 Hz, OCH(CH₃)₂), 3.79 (6H, s, OCH₃), 1.38–1.13, (m, 24 H, OCH(CH₃)₂), 0.92 (d, 12H, *J* = 5.8 Hz, OCH(CH₃)₂). ¹³C NMR (CDCl₃, 50 MHz): δ 159.97 (C=N), 150.64, 150.51, 121.95, 120.17, 119.16, 113.29 (Ar), 78.25, 77.41, 74.51 (OCH(CH₃)₂), 55.59 (OCH₃), 25.88, 25.28, 25.05, 24.05, 23.55 (OCH(CH₃)₂). Anal. Calcd (found) for C₃₄H₅₆N₂O₁₀Ti₂: C, 54.55 (55.05); H, 7.54 (7.49); N, 3.74 (3.76)%. Mp = 122 °C.

Synthesis of $L^{\text{Bu}}\text{-TiOPr}_6$. Using a method similar to that for $L^{\text{H}}\text{-TiOPr}_6$ expect $L^{\text{Bu}}\text{-H}$ was used in place of $L^{\text{H}}\text{-H}$. Yield: 3.42 g (75%). ¹H NMR (CDCl₃, 200 MHz): δ 7.95 (2H, s, CH=N), 7.44, 7.06 (4H, s, Ar-H), 4.95, 4.83, 4.44 (sept, 6H, *J* = 5.8 Hz, OCH(CH₃)₂), 1.52, 1.31 (36H, s, C(CH₃)₃), 1.30–1.08, (m, 24 H, OCH(CH₃)₂), 0.83 (d, 12H, *J* = 5.8 Hz, OCH(CH₃)₂). ¹³C NMR (CDCl₃, 50 MHz): δ 159.29 (C=N), 148.16, 139.11, 137.10, 126.57, 125.44, 120.85 (Ar), 78.09 (OCH(CH₃)₂), 36.01, 33.55 (C(CH₃)₃), 31.55, 29.79 (C(CH₃)₃), 26.02, 22.62, 14.11 (OCH(CH₃)₂). Anal. Calcd (found) for C₄₈H₈₄N₂O₈Ti₂: C, 63.15 (63.74); H, 9.27 (9.73); N, 3.07 (3.31)%. Mp = 133 °C.

Synthesis of $L^{\text{Nap}}\text{-TiOPr}_6$. Using a method similar to that for $L^{\text{H}}\text{-TiOPr}_6$ expect $L^{\text{Nap}}\text{-H}$ was used in place of $L^{\text{H}}\text{-H}$. Yield: 3.35 g (85%). ¹H NMR (CDCl₃, 200 MHz): δ 8.79 (2H, s, CH=N), 7.93, 7.00 (4H, d, *J* = 10 Hz, Ar-H), 7.73, 7.67 (4H, d, *J* = 8 Hz, Ar-H), 7.50, 7.24 (4H, t, *J* = 8 Hz, Ar-H), 4.95, 4.74, 4.41 (sept, 6H, *J* = 5.8 Hz,

OCH(CH₃)₂, 1.33, 1.26, 1.14, 0.82, 0.78 (d, 36H, *J* = 5.8 Hz, OCH(CH₃)₂). ¹³C NMR (CDCl₃, 50 MHz): δ 219.76 (C=N), 165.72, 147.83, 134.61, 133.49, 129.13, 127.40, 123.05, 122.57, 119.73, 110.46 (Ar), 78.60, 78.25, 74.89 (OCH(CH₃)₂), 25.82, 25.46, 25.28, 24.47, 23.52 (OCH(CH₃)₂). Anal. Calcd (found) for C₄₀H₅₆N₂O₈Ti₂: C, 60.92 (60.45); H, 7.16 (7.44); N, 3.55 (3.82) %. Mp = 110 °C.

Synthesis of L^{CH₃}-TiOPr₆. Using a method similar to that for L^H-TiO^{Pr}₆ expect L^{CH₃}-H was used in place of L^H-H. Yield: 2.90 g (81%). ¹H NMR (CDCl₃, 200 MHz): δ 7.33 (2H, t, *J* = 8 Hz, Ar-H), 7.29 (2H, d, *J* = 8 Hz, Ar-H), 6.83 (2H, d, *J* = 8 Hz, Ar-H), 6.74 (2H, t, *J* = 8 Hz, Ar-H), 5.00, 4.77, 4.52 (sept, 6H, *J* = 6.0 Hz, OCH(CH₃)₂), 2.15 (6H, s, CH₃C=N) 1.38, 1.30, 1.20, 1.17, 0.92 (d, 12H, *J* = 6.0 Hz, OCH(CH₃)₂). ¹³C NMR (CDCl₃, 50 MHz): δ 162.92 (C=N), 161.77, 132.21, 128.52, 124.14, 119.63, 116.64 (Ar), 78.75, 77.29, 74.04 (OCH(CH₃)₂), 26.18, 26.08, 25.41, 25.10, 24.23, (OCH(CH₃)₂), 23.57 (CH₃C=N). Anal. Calcd (found) for C₃₄H₅₆N₂O₈Ti₂: C, 56.99 (56.60); H, 7.88 (7.72); N, 3.91 (3.63) %. Mp = 113 °C.

Synthesis of L^{CH₃}-Ti₂O(OPr)₂. 0.12 g of L^{CH₃}-Ti(OPr)₆ was dissolved in CDCl₃ (1.0 mL) in NMR tube. After 2 weeks, only the residual yellow powder was observed in the NMR tube. The crystal of L^{CH₃}-Ti₂O(OPr)₂ was observed from the residual yellow powder.

Synthesis of L^{Br-CH₃}-TiOPr₆. Using a method similar to that for L^H-TiO^{Pr}₆ expect L^{Br-CH₃}-H was used in place of L^H-H. Yield: 2.93 g (67%). ¹H NMR (CDCl₃, 200 MHz): δ 7.40 (2H, s, Ar-H), 7.34, 6.71 (2H, d, *J* = 8 Hz, Ar-H), 4.97, 4.73, 4.51 (sept, 6H, *J* = 6.0 Hz, OCH(CH₃)₂), 2.11 (6H, s, CH₃C=N) 1.36, 1.28, 1.17, 1.14, 0.95, 0.92 (d, 12H, *J* = 6.0 Hz, OCH(CH₃)₂). ¹³C NMR (CDCl₃, 50 MHz): δ 162.01 (C=N), 160.70, 134.94, 130.86, 125.40, 121.61, 107.74 (Ar), 79.21, 77.61, 74.12 (OCH(CH₃)₂), 26.19, 25.30, 25.01, 24.11, 23.43, (OCH(CH₃)₂), 18.41 (CH₃C=N). Anal. Calcd (found) for C₃₄H₅₄Br₂N₂O₈Ti₂: C, 46.71 (46.39); H, 6.23 (6.47); N, 3.20 (3.19) %. Mp = 192 °C.

Synthesis of L^{Ph}-TiOPr₆. Using a method similar to that for L^H-TiO^{Pr}₆ expect L^{Ph}-H was used in place of L^H-H. Yield: 2.90 g (81%). ¹H NMR (CDCl₃, 200 MHz): δ 7.38–7.34 (4H, m, Ar-H), 7.29–7.16 (8H, m, Ar-H), 6.93 (2H, t, *J* = 8 Hz, Ar-H), 6.76 (2H, d, *J* = 8 Hz, Ar-H), 6.49 (2H, t, *J* = 8 Hz, Ar-H), 5.05, 4.76, 4.48 (sept, 6H, *J* = 6.0 Hz, OCH(CH₃)₂), 1.42, 1.36, 1.26, 1.17, 0.90 (d, 12H, *J* = 6.0 Hz, OCH(CH₃)₂). ¹³C NMR (CDCl₃, 50 MHz): δ 162.92 (C=N), 161.77, 132.21, 128.52, 124.14, 119.63, 116.64 (Ar), 78.75, 77.29, 74.04 (OCH(CH₃)₂), 26.18, 26.08, 25.41, 25.10, 24.23, (OCH(CH₃)₂), 23.57 (CH₃C=N). Anal. Calcd (found) for C₄₄H₆₀N₂O₈Ti₂: C, 62.86 (63.10); H, 7.19 (7.52); N, 3.33 (3.93) %. Mp = 121 °C.

Synthesis of L^{Cl-H}-TiOPr₂. A mixture of L^{Cl-H}-H (2.59 g, 10 mmol) and Ti(O^{Pr})₄ (2.843 g, 10 mmol) in THF (30 mL), was stirred for 1 day. Volatile materials were removed under vacuum to give yellow oil and then it was washed with hexane (50 mL). The product precipitated as a yellow powder which was filtered. Yield: 1.64 g (48%). ¹H NMR (CDCl₃, 200 MHz): δ 8.88, 8.08 (4H, s, CH=N), 7.35, 7.25 (8H, d, *J* = 10 Hz, Ar-H), 7.12, 6.27 (4H, d, *J* = 8 Hz, Ar-H), 6.90, 6.61 (4H, t, *J* = 6 Hz, Ar-H), 4.94 (sept, 2H, *J* = 6.0 Hz, OCH(CH₃)₂), 1.24 (d, 12 H, *J* = 6.0 Hz, OCH(CH₃)₂). ¹³C NMR (CDCl₃, 50 MHz): δ 163.37, 161.45 (C=N), 160.59, 136.70, 134.09, 133.66, 132.85, 129.32, 128.63, 120.97, 118.94, 118.12 (Ar), 78.98 (OCH(CH₃)₂), 25.60 (OCH(CH₃)₂). Anal. Calcd (found) for C₃₄H₃₄Cl₂N₄O₄Ti: C, 59.93 (59.54); H, 5.03 (5.08); N, 8.22 (8.72) %. Mp = 148 °C.

Synthesis of ((L^{Cl-H})₃Ti₃O₃). A mixture of L^{Cl-H}-TiOPr₂ (0.53 g, 1.0 mmol) and H₂O (0.18 g, 10 mmol) in THF (30 mL), was stirred for 1 day. Volatile materials were removed under vacuum to give deep yellow oil and then it was washed with hexane (50 mL). The product precipitated as a yellow powder which was filtered. The ¹H NMR spectrum of the yellow powder revealed there were lots of impurities inside and could not further be purified. 0.10 g of the yellow powder was dissolved in CDCl₃ (1.0 mL) in NMR tube. After one month, only the residual yellow powder was observed in the NMR tube. The crystal of ((L^{Cl-H})₃Ti₃O₃) was observed from the residual yellow powder.

General Polymerization Procedures. A typical polymerization procedure was exemplified by the synthesis of entry 1 (Table 1) using complex L^H-TiOPr₆ as a catalyst. The polymerization conversion was analyzed by ¹H NMR spectroscopic studies. Toluene (5.0 mL) was

added to a mixture of complex L^H-TiOPr₆ (0.068 g, 0.1 mmol) and LA (1.44 g, 10 mmol) at 60 °C. After the solution was stirred for 50 min, the reaction was then quenched by adding to a drop of ethanol, and the polymer was precipitated pouring into *n*-hexane (70.0 mL) to give white solids. The white solid was dissolved in CH₂Cl₂ (5.0 mL) and then *n*-hexane (70.0 mL) was added to give white crystalline solid. Yield: 1.08 g (75%).

■ ASSOCIATED CONTENT

Supporting Information

The Supporting Information is available free of charge on the ACS Publications website at DOI: 10.1021/acs.inorgchem.5b02590.

Polymer characterization data, and details of the kinetic study (PDF)

■ AUTHOR INFORMATION

Corresponding Author

*Hsuan-Ying Chen, E-mail: hchen@kmu.edu.tw, Tel.: +886-7-3121101-2585, Fax: +886-7-3125339.

Notes

The authors declare no competing financial interest.

■ ACKNOWLEDGMENTS

This study is supported by Kaohsiung Medical University "Aim for the top 500 universities grant" under Grant No. KMU-DT103007, NSYSU-KMU JOINT RESEARCH PROJECT (#NSYSUKMU 104-P006), and the Ministry of Science and Technology (Grant MOST 104-2113-M-037-010 and 104-2815-C-037-033-M). We thank Center for Research Resources and Development at Kaohsiung Medical University for the instrumentation and equipment support.

■ REFERENCES

- (a) Patel, D.; Moon, J. Y.; Chang, Y.; Kim, T. J.; Lee, G. H. *Colloids Surf., A* **2008**, 313–314, 91–94. (b) Sun, Y.-L.; Chen, Y.-Z.; Wu, R.-J.; Chavali, M.; Huang, Y.-C.; Su, P.-G.; Lin, C.-C. *Sens. Actuators, B* **2007**, 126, 441–446. (c) Raquez, J.-M.; Habibi, Y.; Murariu, M.; Dubois, P. *Prog. Polym. Sci.* **2013**, 38, 1504–1542. (d) Lih, E.; Oh, S. H.; Joung, Y. K.; Leed, J. H.; Han, D. K. *Prog. Polym. Sci.* **2015**, 44, 28–61. (e) Ma, W.-J.; Yuan, X.-B.; Kang, C.-S.; Su, T.; Yuan, X.-Y.; Pu, P.-Y.; Sheng, J. *Carbohydr. Polym.* **2008**, 72, 75–81. (f) Khemtong, C.; Kessinger, C. W.; Gao, J. *Chem. Commun.* **2009**, 3497–3510. (g) Simpson, R. L.; Wiria, F. E.; Amis, A. A.; Chua, C. K.; Leong, K. F.; Hansen, U. N.; Chandrasekaran, M.; Lee, M. W. J. *Biomed. Mater. Res., Part B* **2008**, 84B, 17–25. (h) Place, E. S.; George, J. H.; Williams, C. K.; Stevens, M. M. *Chem. Soc. Rev.* **2009**, 38, 1139–1151. (i) Armentano, I.; Bitinis, N.; Fortunati, E.; Mattioli, S.; Rescignano, N.; Verdejo, R.; Lopez-Manchado, M. A.; Kenny, J. M. *Prog. Polym. Sci.* **2013**, 38, 1720–1747. (j) Thiré, R. M. S. M.; Meiga, T. O.; Dick, S.; Andrade, L. R. *Macromol. Symp.* **2007**, 258, 38–44. (k) Skotak, M.; Leonov, A. P.; Larsen, G.; Noriega, S.; Subramanian, A. *Biomacromolecules* **2008**, 9, 1902–1908. (l) Slomkowski, S. *Macromol. Symp.* **2007**, 253, 47–58. (m) Lickorish, D.; Guan, L.; Davies, J. E. *Biomaterials* **2007**, 28, 1495–1502. (n) Djordjevic, I.; Britcher, L. G.; Kumar, S. *Appl. Surf. Sci.* **2008**, 254, 1929–1935. (o) Wu, W.; Wang, W.; Li, J. *Prog. Polym. Sci.* **2015**, 46, 55–85. (p) Ikada, Y.; Tsuji, H. *Macromol. Rapid Commun.* **2000**, 21, 117–132. (r) Sarpietro, M. G.; Pitarresi, G.; Ottimo, S.; Giuffrida, M. C.; Ognibene, M. C.; Fiorica, C.; Giammona, G.; Castelli, F. *Mol. Pharmaceutics* **2011**, 8, 642–650. (s) Jones, C. H.; Chen, C.-K.; Chen, M.; Ravikrishnan, A.; Zhang, H.; Gollakota, A.; Chung, T.; Cheng, C.; Pfeifer, B. A. *Mol. Pharmaceutics* **2015**, 12, 846–856. (t) (a) Majerska, K.; Duda, A. J. *Am. Chem. Soc.* **2004**, 126, 1026–1027. (b) Sutar, A. K.; Maharana, T.; Dutta, S.; Chen, C.-T.; Lin, C.-C. *Chem. Soc. Rev.* **2010**, 39, 1724–1746. (c) Chisholm, M. H.; Eilerts, N. W.; Huffman, J. C.; Iyer, S. S.; Pacold, M.; Phomphrai, K. J. *Am. Chem. Soc.*

- 2000, 122, 11845–11854. (d) Darensbourg, D. J.; Choi, W.; Karroonnirun, O.; Bhuvanesh, N. *Macromolecules* **2008**, *41*, 3493–3502. (e) O’Keefe, B. J.; Breyfogle, L. E.; Hillmyer, M. A.; Tolman, W. B. *J. Am. Chem. Soc.* **2002**, *124*, 4384–4393. (f) Dove, A. P.; Gibson, V. C.; Marshall, E. L.; Rzepa, H. S.; White, A. J. P.; Williams, D. J. *J. Am. Chem. Soc.* **2006**, *128*, 9834–9843. (g) Williams, C. K.; Breyfogle, L. E.; Choi, S. K.; Nam, W., Jr.; V, G. Y.; Hillmyer, M. A.; Tolman, W. B. *J. Am. Chem. Soc.* **2003**, *125*, 11350–11359. (h) Williams, C. K. *Chem. Soc. Rev.* **2007**, *36*, 1573–1580. (i) Arbaoui, A.; Redshaw, C. *Polym. Chem.* **2010**, *1*, 801–826. (j) Su, C.-K.; Chuang, H.-J.; Li, C.-Y.; Yu, C.-Y.; Ko, B.-T.; Chen, J.-D.; Chen, M.-J. *Organometallics* **2014**, *33*, 7091–7100. (k) Della Monica, F. D.; Luciano, E.; Roviello, G.; Grassi, A.; Milione, S.; Capacchione, C. *Macromolecules* **2014**, *47*, 2830–2841. (l) Chuck, C.-J.; Davidson, M. G.; du Sart, G. G.; Ivanova-Mitseva, P. K.; Kociok-Köhn, G. I.; Manton, L. B. *Inorg. Chem.* **2013**, *52*, 10804–10811. (m) Chang, M.-C.; Lu, W.-Y.; Chang, H.-Y.; Lai, Y.-C.; Chiang, M. Y.; Chen, H.-Y.; Chen, H.-Y. *Inorg. Chem.* **2015**, *54*, 11292–11298. (n) Tabthong, S.; Nanok, T.; Sumrit, P.; Kongsaeere, P.; Prabpai, S.; Chuawong, P.; Hormnirun, P. *Macromolecules* **2015**, *48*, 6846–6861.
- (3) (a) Platel, R. H.; Hodgson, L. M.; Williams, C. K. *Polym. Rev.* **2008**, *48*, 11–63. (b) Arbaoui, A.; Redshaw, C. *Polym. Chem.* **2010**, *1*, 801–826. (c) Stanford, M. J.; Dove, A. P. *Chem. Soc. Rev.* **2010**, *39*, 486–494. (d) Dechy-Cabaret, O.; Martin-Vaca, B.; Bourissou, D. *Chem. Rev.* **2004**, *104*, 6147–6176. (e) O’Keefe, B. J.; Hillmyer, M. A.; Tolman, W. B. *J. Chem. Soc., Dalton Trans.* **2001**, 2215–2224. (f) Gregson, C. K. A.; Gibson, V. C.; Long, N. J.; Marshall, E. L.; Oxford, P. J.; White, A. J. P. *J. Am. Chem. Soc.* **2006**, *128*, 7410–7411. (g) Atkinson, R. C. J.; Gerry, K.; Gibson, V. C.; Long, N. J.; Marshall, E. L.; West, L. J. *Organometallics* **2007**, *26*, 316–320. (h) Lee, J.; Kim, Y.; Do, Y. *Inorg. Chem.* **2007**, *46*, 7701–7703. (i) Chmura, A. J.; Cousins, D. M.; Davidson, M. G.; Jones, M. D.; Lunn, M. D.; Mahon, M. F. *Dalton Trans.* **2008**, 1437–1443. (j) Chen, H.-Y.; Lu, W.-Y.; Chen, Y.-J.; Hsu, S. C. N.; Ou, S.-W.; Peng, W.-T.; Jheng, N.-Y.; Lai, Y.-C.; Wu, B.-S.; Chung, H.; Chen, Y.; Huang, T.-C. *J. Polym. Sci., Part A: Polym. Chem.* **2013**, *51*, 327–333. (k) Sarazin, Y.; Howard, R. H.; Hughes, D. L.; Humphrey, S. M.; Bochmann, M. *Dalton Trans.* **2006**, 340–350. (l) Chen, H.-Y.; Liu, M.-Y.; Sutar, A. K.; Lin, C.-C. *Inorg. Chem.* **2010**, *49*, 665–674. (m) He, J.-X.; Duan, Y.-L.; Kou, X.; Zhang, Y.-Z.; Wang, W.; Yang, Y.; Huang, Y. *Inorg. Chem. Commun.* **2015**, *61*, 144–148.
- (4) Yang, M.; Liu, F. *J. Org. Chem.* **2007**, *72*, 8969–8971.
- (5) Mital, S. P.; Singh, R. V.; Tandon, J. P. *Bull. Chem. Soc. Jpn.* **1982**, *55*, 3653–3654.
- (6) Blout, E. R.; Eager, V. W.; Gofstein, R. M. *J. Am. Chem. Soc.* **1946**, *68*, 1983–1986.
- (7) Wang, L.; Su, Q.; Wu, Q.; Gao, W.; Mu, Y. C. *R. Chim.* **2012**, *15*, 463–470.
- (8) Borsche, W.; Scriba, W. *Justus Liebigs Annalen der Chemie* **1939**, *540*, 83–98.